Transition Metal-centered Trigonal Prisms as Building Units in $RE_{14}T_3In_3$ (RE = Y, Ho, Er, Tm, Lu; T = Pd, Ir, Pt) and Y_4IrIn

Roman Zaremba, Ute Ch. Rodewald, and Rainer Pöttgen

Institut für Anorganische und Analytische Chemie, Universität Münster, Corrensstraße 30, D-48149 Münster, Germany

Reprint requests to R. Pöttgen. E-mail: pottgen@uni-muenster.de

Z. Naturforsch. **2007**, *62b,* 1574 – 1580; received September 19, 2007

The indides $RE_{14}T_3In_3$ (RE = Y, Ho, Er, Tm, Lu; T = Pd, Ir, Pt) and Y_4IrIn were synthesized from the elements by arc-melting and subsequent annealing for crystal growth. Their structures were characterized on the basis of X-ray powder and single crystal data: $Lu_{14}Co_3In_3$-type, space group $P4_2/nmc$, a = 970.2(1), c = 2340.7(5) pm for $Y_{13.95}Pd_3In_{3.05}$, a = 959.7(1), c = 2309.0(5) pm for $Ho_{14}Pd_{2.95}In_3$, a = 955.5(1), c = 2305.1(5) pm for $Er_{14}Pd_3In_3$, a = 950.9(1), c = 2291.6(5) pm for $Tm_{13.90}Pd_3In_{3.10}$, a = 944.4(1), c = 2275.5(5) pm for $Lu_{13.93}Pd_3In_{3.07}$, a = 962.9(1), c = 2343.0(5) pm for $Y_{13.86}Ir_{2.97}In_{3.02}$, a = 967.6(1), c = 2347.8(5) pm for $Y_{13.92}Pt_{3.05}In_{2.91}$, and Gd_4RhIn-type, space group $F\bar{4}3m$, a = 1368.6(2) pm for Y_4IrIn. The main structural motifs are transition metal-centered trigonal prisms of the rare earth elements which are condensed to two-dimensional networks in the $RE_{14}T_3In_3$ indides and to a three-dimensional one in Y_4IrIn. The indium atoms in both structure types show segregation in the metal-rich matrix, *i. e.* In_2 dumbbells in the $RE_{14}T_3In_3$ indides (309 pm In2–In2 in $Y_{13.86}Ir_{2.97}In_{3.02}$) and In_4 tetrahedra (322 pm In–In) in Y_4IrIn. The crystal chemical peculiarities of both structure types are discussed.

Key words: Metal-rich Compounds, Intermetallics, Crystal Structure

Introduction

The rare earth metal-rich parts of the RE-Rh-In systems are governed by four different structure types. The RE_4RhIn indides crystallize with the cubic Gd_4RhIn-type [1]. With slightly higher rare earth content, the $Lu_{14}Co_3In_3$-type [2, 3] compounds $RE_{14}Rh_3In_3$ [4] are obtained. Structural building units of these indides are rhodium-centered trigonal rare earth prisms which are condensed to two- ($Lu_{14}Co_3In_3$-type) and three-dimensional (Gd_4RhIn-type) networks. A different coordination occurs for the series of $RE_3Rh_{2-x}In_x$ compounds [5], where the rhodium atoms have trigonal prismatic and square antiprismatic rare earth coordination. For the smaller scandium atoms, $Sc_{50}Rh_{13.26}In_{2.74}$ has been reported recently [6]. This indide crystallizes with a new structure type. Due to the small size of scandium, the rhodium atoms show coordination numbers 8 and 10.

We have extended the phase analytical investigations of the rare earth metal-rich RE-T-In (T = late transition metal) systems with respect to other transition elements. Herein we report on the new indides $RE_{14}T_3In_3$ (RE = Y, Ho, Er, Tm, Lu; T = Pd, Ir, Pt) and Y_4IrIn.

Table 1. Lattice parameters of the ternary indium compounds $RE_{14}T_3In_3$ (RE = Y, Ho, Er, Tm, Lu, T = Pd, Ir, Pt) and Y_4IrIn.

Starting / Refined composition (Guinier powder / single crystal data)		a (pm)	c (pm)	V (nm^3)
14Y:3Pd:3In /		971.5(7)	2343(1)	2.2114
	$Y_{13.95}Pd_3In_{3.05}$	970.2(1)	2340.7(5)	2.2033
14Ho:3Pd:3In /		959.9(7)	2300(3)	2.1192
	$Ho_{14}Pd_{2.95}In_3$	959.7(1)	2309.0(5)	2.1266
14Er:3Pd:3In /		955.6(3)	2300(2)	2.1003
	$Er_{14}Pd_3In_3$	955.5(1)	2305.1(5)	2.1045
14Tm:3Pd:3In /		950.8(4)	2285(1)	2.0657
	$Tm_{13.90}Pd_3In_{3.10}$	950.9(1)	2291.6(5)	2.0720
14Lu:3Pd:3In /		944.1(4)	2278.4(9)	2.0308
	$Lu_{13.93}Pd_3In_{3.07}$	944.4(1)	2275.5(5)	2.0295
14Y:3Ir:3In /		963.6(2)	2345.0(7)	2.1774
	$Y_{13.86}Ir_{2.97}In_{3.02}$	962.9(1)	2343.0(5)	2.1724
14Y:3Pt:3In /		967.2(3)	2344(1)	2.1928
	$Y_{13.92}Pt_{3.05}In_{2.91}$	967.6(1)	2347.8(5)	2.1981
14Y:3Ir:3In /		1368.8(8)	a	2.5646
	Y_4IrIn	1368.6(2)	a	2.5635

Experimental Section

Synthesis

Starting materials for the preparation of the indides $RE_{14}T_3In_3$ (RE = Y, Ho, Er, Tm, Lu, T = Pd, Ir and Pt) and Y_4IrIn were ingots of the rare earth elements (John-

Table 2. Crystal data and structure refinement for $Y_{13.95(1)}Pd_3In_{3.05(1)}$, $Ho_{14}Pd_{2.95(1)}In_3$, $Er_{14}Pd_3In_3$, $Tm_{13.90(1)}Pd_3In_{3.10(1)}$ and $Lu_{13.93(1)}Pd_3In_{3.07(1)}$, space group $P4_2/nmc$, $Z = 4$.

Empirical formula	$Y_{13.95(1)}Pd_3In_{3.05(1)}$	$Ho_{14}Pd_{2.95(1)}In_3$	$Er_{14}Pd_3In_3$	$Tm_{13.90(1)}Pd_3In_{3.10(1)}$	$Lu_{13.93(1)}Pd_3In_{3.07(1)}$
Molar mass, g/mol	1909.70	2967.09	3005.30	3023.00	3109.03
Unit cell dimensions	see Table 1	see Table 1	see Table 1	see Table 1	see Table 1
Calculated density, g cm^{-3}	5.76	9.27	9.49	9.69	10.18
Crystal size, μm^3	$20 \times 60 \times 170$	$20 \times 70 \times 80$	$10 \times 40 \times 70$	$20 \times 40 \times 60$	$40 \times 50 \times 160$
Detector distance, mm	80	60	80	80	90
Exposure time, min	4	5	5	5	4
ω Range; increment, deg	0 – 180; 1.0	0 – 180; 1.0	0 – 180; 1.0	0 – 180; 1.0	0 – 180; 1.0
Integr. param. A; B; EMS	13.5; 3.5; 0.012	13.0; 3.0; 0.014	13.0; 3.0; 0.012	13.5; 3.5; 0.012	13.5; 3.5; 0.012
Transm. ratio (max/min)	6.96	3.91	2.44	5.33	11.40
Absorption coeff., mm^{-1}	41.7	56.9	60.8	64.6	73.0
F(000), e	3326	4882	4948	4996	5110
θ Range, deg	2 – 30	2 – 30	2 – 32	2 – 30	2 – 30
Range in *hkl*	−13/12, ±13, −32/29	±12, ±13, ±31	−12/14, −13/14, ±34	±13, ±13, −32/29	±12, ±13, ±32
Total no. reflections	21987	19555	24359	20550	20304
Independent reflections	1790 (R_{int} = 0.134)	1606 (R_{int} = 0.081)	2000 (R_{int} = 0.144)	1681 (R_{int} = 0.171)	1655 (R_{int} = 0.099)
Reflections with $I \geq 2\sigma(I)$	1068 (R_σ = 0.101)	1088 (R_σ = 0.060)	1028 (R_σ = 0.137)	791 (R_σ = 0.165)	1074 (R_σ = 0.068)
Data/parameters	1790 / 63	1606 / 63	2000 / 62	1681 / 63	1655 / 63
Goodness-of-fit on F^2	0.698	0.756	0.636	0.548	0.724
Final R indices	$R1$ = 0.030	$R1$ = 0.024	$R1$ = 0.029	$R1$ = 0.028	$R1$ = 0.024
$[I \geq 2\sigma(I)]$	$wR2$ = 0.047	$wR2$ = 0.042	$wR2$ = 0.048	$wR2$ = 0.039	$wR2$ = 0.047
R indices (all data)	$R1$ = 0.072	$R1$ = 0.045	$R1$ = 0.090	$R1$ = 0.087	$R1$ = 0.047
	$wR2$ = 0.052	$wR2$ = 0.044	$wR2$ = 0.055	$wR2$ = 0.045	$wR2$ = 0.050
Extinction coefficient	0.00077(2)	0.000523(13)	0.000269(8)	0.000263(8)	0.000270(9)
Largest diff. peak and hole, e Å^{-3}	4.82 / −1.52	4.99 / −2.17	4.17 / −2.57	3.33 / −2.45	3.14 / −3.04

Table 3. Crystal data and structure refinement for $Y_{13.86(1)}Ir_{2.97(1)}In_{3.02(1)}$ and $Y_{13.92(1)}Pt_{3.05(1)}In_{2.91(1)}$, space group $P4_2/nmc$, $Z = 4$, Y_4IrIn, space group $F\bar{4}3m$, $Z = 16$.

Empirical formula	$Y_{13.86(1)}Ir_{2.97(1)}In_{3.02(1)}$	$Y_{13.92(1)}Pt_{3.05(1)}In_{2.91(1)}$	Y_4IrIn
Molar mass, g/mol	2150.65	2166.69	662.66
Unit cell dimensions	see Table 1	see Table 1	see Table 1
Calculated density, g cm^{-3}	6.58	6.55	6.87
Crystal size, μm^3	$30 \times 40 \times 100$	$30 \times 100 \times 160$	$30 \times 30 \times 100$
Detector distance, mm	80	80	100
Exposure time, min	5	4	15
ω Range; increment, deg	0 – 180; 1.0	0 – 180; 1.0	0 – 180; 1.0
Integr. param. A; B; EMS	13.5; 3.5; 0.014	13.5; 3.5; 0.012	13.0; 3.0; 0.014
Transm. ratio (max/min)	4.28	11.42	4.32
Absorption coefficient, mm^{-1}	57.7	58.5	59.8
F(000), e	3670	3693	4512
θ Range, deg	2 – 32	2 – 30	2 – 30
Range in *hkl*	±14, ±14, −33/34	±13, ±13, ±32	−16/18, −17/18, ±18
Total no. reflections	24659	22099	5260
Independent reflections	2064 (R_{int} = 0.213)	1772 (R_{int} = 0.176)	395 (R_{int} = 0.213)
Reflections with $I \geq 2\sigma(I)$	861 (R_σ = 0.249)	1152 (R_σ = 0.109)	272 (R_σ = 0.143)
Data/parameters	2064 / 65	1772 / 65	395 / 20
Goodness-of-fit on F^2	0.476	0.766	0.588
Final R indices $[I \geq 2\sigma(I)]$	$R1$ = 0.032	$R1$ = 0.034	$R1$ = 0.033
	$wR2$ = 0.045	$wR2$ = 0.061	$wR2$ = 0.050
R indices (all data)	$R1$ = 0.108	$R1$ = 0.065	$R1$ = 0.057
	$wR2$ = 0.056	$wR2$ = 0.065	$wR2$ = 0.055
Extinction coefficient	0.000304(9)	0.00065(3)	0.000112(10)
Flack parameter	–	–	0.36(3)
Largest diff. peak and hole, e Å^{-3}	2.15 / −2.22	5.11 / −2.09	1.92 / −1.37

Table 4. Atomic coordinates and isotropic displacement parameters (pm^2) of $RE_{14}T_3In_3$ (*RE* = Y, Ho, Er, Tm, Lu, *T* = Pd, Ir, Pt) and Y_4IrIn. U_{eq} is defined as one third of the trace of the orthogonalized U_{ij} tensor.

Atom	Wyckoff site	Occupancy, %	*x*	*y*	*z*	U_{eq}
$Y_{13.95(1)}Pd_3In_{3.05(1)}$						
Y1/In3	4*c*	94(2)/6(2)	3/4	1/4	0.14593(7)	81(5)
Y2	4*d*	100	1/4	1/4	0.21395(7)	71(3)
Y3	8*g*	100	1/4	0.54069(13)	0.30858(5)	96(2)
Y4	8*g*	100	1/4	0.56432(12)	0.98430(4)	75(2)
Y5	8*f*	100	0.56540(7)	$-x$	1/4	68(2)
Y6	8*g*	100	1/4	0.44312(12)	0.46550(5)	76(2)
Y7	16*h*	100	0.44097(8)	0.43561(9)	0.10447(3)	63(1)
Pd1	8*g*	100	1/4	0.53681(10)	0.18968(4)	85(2)
Pd2	4*d*	100	1/4	1/4	0.55353(5)	69(2)
In1	4*c*	100	3/4	1/4	0.90852(5)	90(2)
In2	8*g*	100	1/4	0.41284(9)	0.85494(4)	71(2)
$Ho_{14}Pd_{2.95(1)}In_3$						
Ho1	4*c*	100	3/4	1/4	0.14513(4)	88(2)
Ho2	4*d*	100	1/4	1/4	0.21417(4)	89(2)
Ho3	8*g*	100	1/4	0.54112(7)	0.30995(3)	112(2)
Ho4	8*g*	100	1/4	0.56484(7)	0.98525(3)	97(1)
Ho5	8*f*	100	0.56593(4)	$-x$	1/4	86(1)
Ho6	8*g*	100	1/4	0.44511(7)	0.46520(3)	90(1)
Ho7	16*h*	100	0.44362(5)	0.43552(5)	0.10397(2)	80(1)
Pd1	8*g*	97.4(6)	1/4	0.53642(12)	0.18980(5)	89(4)
Pd2	4*d*	100	1/4	1/4	0.55380(7)	87(3)
In1	4*c*	100	3/4	1/4	0.90913(7)	125(3)
In2	8*g*	100	1/4	0.41145(10)	0.85520(5)	83(2)
$Er_{14}Pd_3In_3$						
Er1	4*c*	100	3/4	1/4	0.14512(6)	75(2)
Er2	4*d*	100	1/4	1/4	0.21388(6)	76(2)
Er3	8*g*	100	1/4	0.53995(11)	0.30962(4)	92(2)
Er4	8*g*	100	1/4	0.56432(11)	0.98497(4)	79(2)
Er5	8*f*	100	0.56603(7)	$-x$	1/4	72(2)
Er6	8*g*	100	1/4	0.44506(11)	0.46521(4)	73(2)
Er7	16*h*	100	0.44353(7)	0.43533(8)	0.10415(2)	64(1)
Pd1	8*g*	100	1/4	0.53694(18)	0.18985(7)	80(3)
Pd2	4*d*	100	1/4	1/4	0.55375(9)	63(4)
In1	4*c*	100	3/4	1/4	0.90895(9)	93(4)
In2	8*g*	100	1/4	0.41212(15)	0.85519(7)	56(3)
$Tm_{13.90(1)}Pd_3In_{3.10(1)}$						
Tm1/In3	4*c*	90(2)/10(2)	3/4	1/4	0.14508(7)	57(5)
Tm2	4*d*	100	1/4	1/4	0.21384(6)	60(3)
Tm3	8*g*	100	1/4	0.53952(13)	0.30970(5)	83(2)
Tm4	8*g*	100	1/4	0.56403(13)	0.98499(4)	70(2)
Tm5	8*f*	100	0.56600(8)	$-x$	1/4	61(2)
Tm6	8*g*	100	1/4	0.44529(12)	0.46518(5)	61(2)
Tm7	16*h*	100	0.44376(8)	0.43530(9)	0.10427(3)	52(1)
Pd1	8*g*	100	1/4	0.5366(2)	0.18988(8)	67(4)
Pd2	4*d*	100	1/4	1/4	0.55361(10)	45(5)
In1	4*c*	100	3/4	1/4	0.90895(10)	88(5)
In2	8*g*	100	1/4	0.41266(17)	0.85508(8)	50(3)
$Lu_{13.93(1)}Rh_3In_{3.07(1)}$						
Lu1/In3	4*c*	94(2)/6(2)	3/4	1/4	0.14495(5)	85(4)
Lu2	4*d*	100	1/4	1/4	0.21380(5)	76(2)
Lu3	8*g*	100	1/4	0.53945(8)	0.31026(3)	101(2)
Lu4	8*g*	100	1/4	0.56330(8)	0.98510(3)	83(1)
Lu5	8*f*	100	0.56540(5)	$-x$	1/4	76(1)
Lu6	8*g*	100	1/4	0.44579(8)	0.46523(3)	75(1)
Lu7	16*h*	100	0.44321(5)	0.43536(5)	0.10439(2)	68(1)

Table 4 (continued).

Atom	Wyckoff site	Occupancy, %	x	y	z	U_{eq}
Pd1	8*g*	100	1/4	0.53697(14)	0.19038(6)	87(3)
Pd2	4*d*	100	1/4	1/4	0.55356(8)	65(3)
In1	4*c*	100	3/4	1/4	0.90915(7)	93(3)
In2	8*g*	100	1/4	0.41359(12)	0.85529(6)	69(2)
$Y_{13.86(1)}Ir_{2.97(1)}In_{3.02(1)}$						
Y1/In3	4*c*	86(3)/14(3)	3/4	1/4	0.14627(10)	95(7)
Y2	4*d*	100	1/4	1/4	0.21575(10)	81(5)
Y3	8*g*	100	1/4	0.5508(2)	0.30717(8)	103(4)
Y4	8*g*	100	1/4	0.5591(2)	0.98428(6)	86(4)
Y5	8*f*	100	0.55912(13)	$-x$	1/4	117(4)
Y6	8*g*	100	1/4	0.44325(19)	0.46547(7)	74(3)
Y7	16*h*	100	0.43703(14)	0.43408(15)	0.10478(4)	74(2)
Ir1	8*g*	92.8(4)	1/4	0.52970(8)	0.18995(3)	97(2)
Ir2	4*d*	100	1/4	1/4	0.54968(4)	86(2)
In1/Ir3	4*c*	88(1)/12(1)	3/4	1/4	0.91023(7)	89(6)
In2	8*g*	100	1/4	0.41066(14)	0.85455(5)	74(3)
$Y_{13.92(1)}Pt_{3.05(1)}In_{2.91(1)}$						
Y1/In3	4*c*	92(3)/8(3)	3/4	1/4	0.14619(9)	96(6)
Y2	4*d*	100	1/4	1/4	0.21411(9)	82(4)
Y3	8*g*	100	1/4	0.54307(14)	0.30779(7)	104(3)
Y4	8*g*	100	1/4	0.56188(14)	0.98383(7)	94(3)
Y5	8*f*	100	0.56388(9)	$-x$	1/4	96(3)
Y6	8*g*	100	1/4	0.44321(14)	0.46518(7)	90(3)
Y7	16*h*	100	0.43838(10)	0.43500(10)	0.10498(5)	77(2)
Pt1	8*g*	93.9(3)	1/4	0.53403(6)	0.19037(3)	82(2)
Pt2	4*d*	100	1/4	1/4	0.55168(4)	87(2)
In1/Pt3	4*c*	83(1)/17(1)	3/4	1/4	0.90945(6)	110(5)
In2	8*g*	100	1/4	0.41245(11)	0.85459(5)	87(2)
Y_4IrIn						
Y1	24*g*	100	0.4405(2)	3/4	3/4	107(6)
Y2	24*f*	100	0.8086(2)	0	0	74(7)
Y3	16*e*	100	0.65156(15)	x	x	84(7)
Ir	16*e*	100	0.85896(6)	x	x	91(3)
In	16*e*	100	0.41685(12)	x	x	108(6)

son Matthey, Chempur or Kelpin), palladium, iridium and platinum powder (Merck, Heraeus), and indium tear drops (Merck), all with stated purities better than 99.9 %. In a first step, the rare earth metal pieces were arc-melted [7] under 600 mbar argon to small buttons. The argon was purified with titanium sponge (900 K), silica gel, and molecular sieves. The pre-melting procedure reduces shattering during the subsequent reactions with the transition elements and indium. Pieces of the respective rare earth and transition metal (cold-pressed to pellets of 6 mm diameter) and pieces of the indium tear drops were mixed in the 14 : 3 : 3 atomic ratio. The mixtures were reacted in the arc-furnace and remelted three times to ensure homogeneity. The weight losses after the arc-melting procedures were always smaller than 0.5 %. The light gray polycrystalline samples are brittle and stable in air over months. Powders are dark gray and single crystals exhibit metallic luster. $Y_{14}Ir_3In_3$ was prepared by induction melting of a 14 : 3 : 3 mixture in a tantalum crucible [8]. The reaction mixture was rapidly heated under argon to 1700 K, cooled to 1000 K and kept at that temperature for another 2 h followed by quenching to r. t.

Single crystals of the indides $RE_{14}T_3In_3$ (*RE* = Y, Ho, Er, Tm, Lu, *T* = Pd, and Pt) were grown *via* a special annealing sequence. The arc-melted polycrystalline samples were first powdered and cold-pressed into small pellets (⌀ 6 mm). Next, the pellets were put in small tantalum containers that were sealed in evacuated silica tubes as an oxidation protection. The ampoules were first heated to 1320 K within 6 h and held at this temperature for another 6 h. Subsequently, the temperature was lowered by 5 K/h to 970 K in all cases, then at a rate of 15 K/h to 670 K. Finally the samples were cooled to r. t. by switching off the furnace. The products could easily be separated from the tantalum containers. No reaction of the samples with tantalum could be detected. $RE_{14}T_3In_3$ single crystals of irregular shape were selected. The Y_4IrIn single crystal was taken from an $Y_{14}Ir_3In_3$ sample as a byproduct.

Table 5. Interatomic distances (pm), calculated with the powder lattice parameters of $Y_{13.86(1)}Ir_{2.97(1)}In_{3.02(1)}$ and Y_4IrIn. All distances within the first coordination spheres are listed. Standard deviationas are all equal or smaller than 0.2 pm.

$Y_{13.86(1)}Ir_{2.97(1)}In_{3.02(1)}$											
Y1/In3:	2	In2	326.8	Y5:	2	In2	338.0	Ir1:	1	Y3	275.4
	4	Y5	355.9		2	Ir1	340.2		1	Y2	276.0
	2	Y4	356.9		2	Y3	343.1		2	Y7	284.1
	4	Y7	362.9		2	Y1/In3	355.9		2	Y3	286.1
Y2:	2	Ir1	276.0		2	Y2	358.9		1	In1/Ir3	316.4
	4	Y5	358.9		2	Y7	360.1		2	Y5	340.2
	2	In2	360.1		2	Y5	367.6	Ir2:	2	Y6	271.2
	2	Y3	360.2	Y6:	1	Ir2	271.2		4	Y7	283.8
	4	Y7	362.6		1	In1/Ir3	322.5		2	Y4	334.7
	1	Ir2	389.1		2	Y4	353.7		1	Y2	389.1
Y3:	1	Ir1	275.4		2	In2	355.1	In1/Ir3:	2	Y4	308.1
	2	Ir1	286.1		2	Y7	364.6		2	Y3	308.4
	1	In1/Ir3	308.4		2	Y4	367.3		2	Ir1	316.4
	2	Y5	343.1		2	Y7	371.5		2	Y6	322.5
	2	In2	346.6		1	Y6	372.2		4	Y7	355.3
	1	Y2	360.2		1	Y3	385.1	In2:	1	In2	309.4
	2	Y7	367.8	Y7:	1	Ir2	283.8		1	Y1/In3	326.8
	2	Y3	381.3		1	Ir1	284.1		1	Y4	335.9
	1	Y3	383.6		1	In2	349.6		2	Y5	338.0
	1	Y6	385.1		1	Y7	354.5		2	Y3	346.6
Y4:	1	In1/Ir3	308.1		1	In1/Ir3	355.3		2	Y7	349.6
	1	Ir2	334.7		1	Y4	355.8		2	Y6	355.1
	1	In2	335.9		1	Y5	360.1		1	Y2	360.1
	2	Y6	353.7		1	Y7	360.2				
	2	Y7	355.8		1	Y2	362.6				
	1	Y1/In3	356.9		1	Y1/In3	362.9				
	2	Y7	366.6		1	Y6	364.6				
	2	Y6	367.3		1	Y4	366.6				
	1	Y4	367.7		1	Y3	367.8				
					1	Y6	371.5				
Y_4IrIn											
Y1:	2	In	324.6	Y3:	3	Ir	284.6	In:	3	In	321.9
	2	Y3	346.0		3	Y1	346.0		3	Y1	324.6
	2	Ir	346.1		3	In	347.5		3	Y3	347.5
	4	Y2	360.8		3	Y2	363.7		3	Y2	348.0
	4	Y1	368.8		3	Y3	381.1				
Y2:	2	Ir	281.6	Ir:	3	Y2	281.6				
	2	In	348.0		3	Y3	284.6				
	4	Y1	360.8		3	Y1	346.1				
	2	Y3	363.7								
	4	Y2	370.6								

X-Ray diffraction

All samples were analyzed *via* Guinier powder patterns (imaging plate technique, Fujifilm BAS-1800) using CuK_{α_1} radiation and α-quartz (a = 491.30 and c = 540.46 pm) as an internal standard. The lattice parameters (Table 1) were obtained from least-squares fits of the powder data. To ensure correct indexing, the experimental patterns were compared with calculated ones [9], taking the atomic positions from the structure refinements.

Single crystal intensity data of several crystals were collected at r. t. on a Stoe IPDS-II image plate system in oscillation mode. Numerical absorption corrections were applied to the data sets. All relevant details concerning the data collections are listed in Tables 2 and 3.

Structure refinements

Small, irregularly shaped single crystals of the indides $RE_{14}T_3In_3$ and Y_4IrIn were selected from the annealed samples by mechanical fragmentation and examined by use of a Buerger camera equipped with an image plate system (Fujifilm BAS-1800) in order to establish suitability for intensity data collection. The $RE_{14}T_3In_3$ data sets were compatible with space group $P4_2/nmc$ and the ones of Y_4IrIn with space group $F\bar{4}3m$, in agreement with our previous investigations [4, 10].

The atomic positions of $Y_{14}Rh_3In_3$ [4] and Gd_4IrIn [10] were taken as starting parameters and the structures were refined using SHELXL-97 [11] (full-matrix least-squares on F^2) with anisotropic atomic displacement parameters for all atoms. Similar to the series $RE_{14}Co_3In_3$ [2, 3], $RE_{14}Ni_3In_3$

[12], and $RE_{14}Rh_3In_3$ [4], the $RE_{14}T_3In_3$ compounds presented here also revealed some mixed occupied sites or small defects, leading to the refined compositions listed in Table 4. The Y_4IrIn crystal showed twinning by inversion. The final difference Fourier syntheses were flat (Tables 2 and 3). The positional parameters and interatomic distances (exemplarily for $Y_{13.86}Ir_{2.97}In_{3.02}$ and Y_4IrIn) of the refinements are listed in Tables 4 and 5. Further details of the crystal structure investigation may be obtained from Fachinformationszentrum Karlsruhe, 76344 Eggenstein-Leopoldshafen, Germany (fax: +49-7247-808-666; e-mail: crysdata@fiz-karlsruhe.de, http://www.fiz-informationsdienste.de/en/DB/icsd/depot_anforderung.html) on quoting the deposition numbers CSD-418561 ($Y_{13.95}Pd_3In_{3.05}$), CSD-418565 ($Ho_{14}Pd_{2.95}In_3$), CSD-418560 ($Er_{14}Pd_3In_3$), CSD-418564 ($Tm_{13.90}Pd_3In_{3.10}$), CSD-418566 ($Lu_{13.93}Rh_3In_{3.07}$), CSD-418562 ($Y_{13.86}Ir_{2.97}In_{3.02}$), CSD-418563 ($Y_{13.92}Pt_{3.05}In_{2.91}$), and CSD-418567 ($Y_4IrIn$).

Scanning electron microscopy

The bulk samples and the single crystals of the indides $RE_{14}T_3In_3$ and Y_4IrIn were analyzed in a LEICA 420 I scanning electron microscope equipped with an OXFORD EDX analyzer. Since the crystals were mounted by beeswax on glass fibres, they were first coated with a carbon film. The bulk samples were embedded in a methacrylate matrix and the surface was polished with different silica and diamond pastes. The surface remained unetched for the EDX measurements. The rare earth trifluorides, Pd, Ir, Pt, and InAs were used as standards for the semiquantitative analyses. The compositions determined by EDX were close to the ideal compositions. No impurity elements were observed.

Results and Discussion

The indides $RE_{14}T_3In_3$ and Y_4IrIn are new members in the families of $Lu_{14}Co_3In_3$- [2, 3] and Gd_4RhIn-type [1] compounds. These two structure types are very close in composition and they exhibit similar structural features. The structural chemistry of these two structure types has been discussed in detail previously [1 – 4, 10] and we therefore refer to the literature. Herein, we exemplarily discuss the common structural features of $Y_{13.86}Ir_{2.97}In_{3.02}$ and Y_4IrIn.

The iridium atoms in both structures have trigonal prismatic yttrium coordination. The Ir–Y distances range from 271 – 286 pm in $Y_{13.86}Ir_{2.97}In_{3.02}$ and from 282 – 285 pm in Y_4IrIn. These distances are all smaller than the sum of the covalent radii of 288 pm [13], indicating strong Y–Ir bonding in

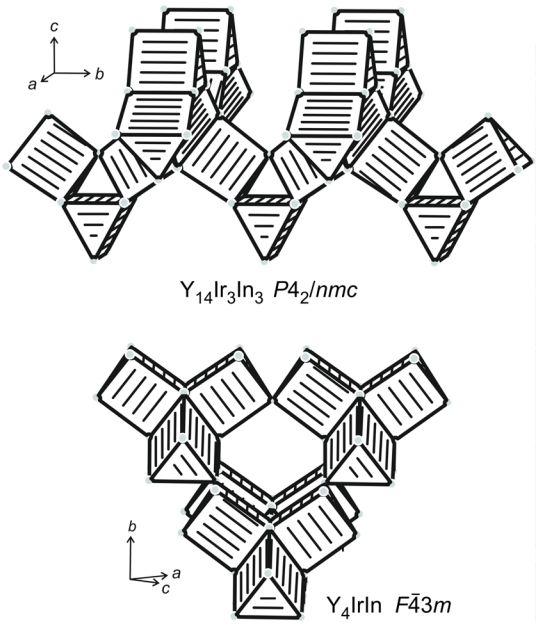

Fig. 1. Cutouts of the structures of $Y_{13.86(1)}Ir_{2.97(1)}In_{3.02(1)}$ and Y_4IrIn. The linkage of the iridium-centered trigonal prisms of yttrium atoms is emphasized.

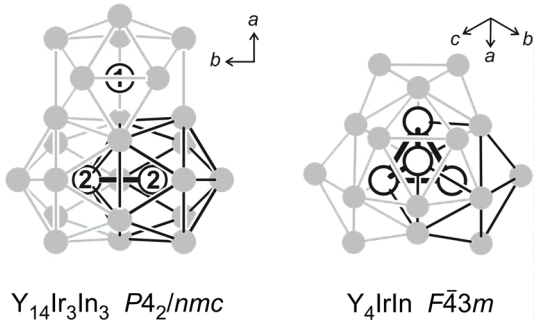

Fig. 2. Cutouts of the $Y_{13.86(1)}Ir_{2.97(1)}In_{3.02(1)}$ and Y_4IrIn structures, emphasizing the indium substructures. In each drawing, one distorted icosahedron around indium is emphasized. Yttrium and indium atoms are drawn as medium grey and open circles, respectively.

$Y_{13.86}Ir_{2.97}In_{3.02}$ and Y_4IrIn. The trigonal prisms are condensed *via* common edges and corners to a two-dimensional network in $Y_{13.86}Ir_{2.97}In_{3.02}$ and to a three-dimensional one in Y_4IrIn. Cutouts of the different linkages are presented in Fig. 1.

In both structures we observe a segregation of the indium atoms, *i. e.* $In2_2$ pairs (309 pm In–In) in $Y_{13.86}Ir_{2.97}In_{3.02}$ and In_4 tetrahedra (322 pm In–In) in Y_4IrIn. Both distances are smaller than in tetragonal body-centered indium (4×325 and 8×338 pm) [14].

The cutouts of the $Y_{13.86}Ir_{2.97}In_{3.02}$ and Y_4IrIn structures presented in Fig. 2 emphasize the yttrium coordination of the indium atoms. In both structures, the indium atoms of the $In2_2$ dumbbells and those of the In_4 tetrahedra have distorted icosahedral yttrium coordination. These icosahedra interpenetrate, leading to the double unit in $Y_{13.86}Ir_{2.97}In_{3.02}$ and the quadruple unit in Y_4IrIn. Thus, the indium subunits are well embedded in the yttrium matrices. The Y–Y distances range from 343 to 385 and from 346 to 381 pm in $Y_{13.86}Ir_{2.97}In_{3.02}$ and Y_4IrIn, respectively. Several of these distances are shorter than in *hcp* yttrium (6×356 and 6×364 pm) [14], suggesting substantial Y–Y bonding.

Acknowledgement

This work was financially supported by the Deutsche Forschungsgemeinschaft.

[1] R. Zaremba, U. Ch. Rodewald, R.-D. Hoffmann, R. Pöttgen, *Monatsh. Chem*. **2007**, *138*, 523.
[2] V. I. Zaremba, Ya. M. Kalychak, P. Yu. Zavalii, *Sov. Phys. Crystallogr*. **1992**, *37*, 178.
[3] V. I. Zaremba, Ya. M. Kalychak, M. V. Dzevenko, U. Ch. Rodewald, B. Heying, R. Pöttgen, *Z. Naturforsch*. **2006**, *61b*, 23.
[4] R. Zaremba, R. Pöttgen, *J. Solid State Chem*. **2007**, *180*, 2452.
[5] R. Zaremba, U. Ch. Rodewald, V. I. Zaremba, R. Pöttgen, *Z. Naturforsch*. in press.
[6] R. Zaremba, R. Pöttgen, *Z. Naturforsch*. **2007**, *62b*, 1567.
[7] R. Pöttgen, Th. Gulden, A. Simon, *GIT Labor-Fachzeitschrift* **1999**, 4*3*, 133.
[8] D. Kußmann, R.-D. Hoffmann, R. Pöttgen, *Z. Anorg. Allg. Chem*. **1998**, *624*, 1727.
[9] K. Yvon, W. Jeitschko, E. Parthé, *J. Appl. Crystallogr*. **1977**, *10*, 73.
[10] R. Zaremba, U. Ch. Rodewald, R.-D. Hoffmann, R. Pöttgen, *Monatsh. Chem*., in press.
[11] G. M. Sheldrick, SHELXL-97, Program for Crystal Structure Refinement, University of Göttingen, Göttingen (Germany) **1997**.
[12] M. Lukachuk, Ya. V. Galadzhun, R. I. Zaremba, M. V. Dzevenko, Ya. M. Kalychak, V. I. Zaremba, U. Ch. Rodewald, R. Pöttgen, *J. Solid State Chem*. **2005**, *178*, 2724.
[13] J. Emsley, *The Elements*, Oxford University Press, Oxford, **1999**.
[14] J. Donohue, *The Structures of the Elements*, Wiley, New York, **1974**.